MAJOR AVALANCHES OCCURRENCE AT REGIONAL SCALE AND RELATED ATMOSPHERIC CIRCULATION PATTERNS IN THE EASTERN PYRENEES

Carles García* (1), Glòria Martí (1), Pere Oller (1), Ivan Moner (2), Jordi Gavaldà (2), Pere Martínez (1), Juan Carlos Peña (3)

(1) Institut Geològic de Catalunya, Barcelona, Spain

(2) Conselh Generau d'Aran, Vielha, Spain

(3) Servei Meteorològic de Catalunya, Spain

ABSTRACT: The occurrence of major avalanche episodes in the Eastern Pyrenees (NE Spain) is estimated by means of the Poisson and the negative binomial distributions, assuming that they are rare events. Occurrence fits better the Poisson distribution provided that the avalanche episodes are independent. The differences observed in the spatial distribution of major avalanche episodes, within the seven regions in which Eastern Pyrenees were divided, suggest us to look for spatial variations in the relationship between extreme avalanche episodes and synoptic-scale atmospheric circulation patterns. By applying principal-component analysis procedure, six atmospheric patterns leading to major avalanches were obtained at 500 hPa geopotential height. Next, the atmospheric pressure deviation of each component is calculated with respect to the average atmospheric circulation to assess the abnormality of atmospheric patterns leading major avalanches in the Pyrenees. The pressure anomaly maps give also an idea of the role that the North Atlantic Oscillation index (NAOi) plays in the occurrence of extreme avalanche episodes in the Eastern Pyrenees.

* *Corresponding author address*: Carles García Sellés, Institut Geològic de Catalunya, C/Balmes 209-211, BCN 08006, Spain; tel: 0034 935538426; fax: 0034 935538436; email: cgarcia@igc.cat.

The interest of connecting major avalanche episodes with NAOi lies in the fact of this low-frequency pattern seems to be predictable at medium term for the next winter with a reasonable level of confidence. The accuracy of regional avalanche warning is expected to increase by means of the proposed methodology. It should reduce the trend to overestimate the avalanche danger level when forecasting is based on expected critical snow depth. This procedure is especially suitable for regions where long term snow-climate databases do not exist and avalanche warning is strongly supported on meteorological forecasting models.

KEY WORDS: major avalanches, atmospheric patterns, principal-component analysis, Pyrenees.

1. INTRODUCTION

In the Eastern Pyrenees (NE Spain), the growth of tourism in recent decades has resulted in an increase of house building, opening of mountain roads during winter, and a spread of associated infrastructures. New ski resorts are expected to be built and to be enlarged. As a consequence, exposure to natural hazards is increasing and so is the risk. The number of skiers and mountaineers killed by avalanches has grown in the last years (Martínez et al., 2004). Studies dealing with avalanche conditions at the Pyrenees are very scarce, and usually on very specific cases. Therefore, this article tries to open a new line of enquiry on atmospheric conditions and regional forecasting of major avalanches.

Frequently, the occurrence of rare events in meteorological phenomenon has been analysed by applying the Poisson and the negative binomial distributions (Thom, 1966; Sakamoto, 1973). Our paper applies these models to the annual probability of major avalanches episodes, considering major avalanches episode as a discrete natural event (Hewit, 1970). For snow avalanches, Poisson distribution has been used to model the arrival rate of avalanches (McCLung, 2000), and the use of probability models for computation of design return periods, magnitudes and frequencies of avalanches has been recently reviewed (Eckert et al., 2007).

Relationships between avalanches, meteorological conditions and climate have been thoroughly studied. A lot of research in this field has been undertaken in the United States and

Canada. Pioneering studies relating avalanches activity to climate in a regional scale had been performed by LaChapelle (1966), Schaerer (1986) and Armstrong and Armstrong (1987). Studies for specific sites that analyse the relationship between regional atmospheric circulation patterns and avalanche data have been undertaken by Fitzharris (1981) and Mock (1996). More recently, Birkeland et al. (2001) has emphasized that differences in avalanche activity with distinctive atmospheric conditions can be observed even in sites located in a similar avalanche climate. His conclusions remark that local topography explains different effects of synoptic patterns on avalanches.

Studies developed by Hächler (1987) at the Swiss Alps take into account circulation patterns to explain major avalanches in a regional scale. He differentiated circulation patterns that generated severe avalanches in the Northern and Southern Alps. He focused on both, geographical factors such as distance from the nearest sea, mountains disposition, and dynamic factors such as the direction of the upper-level airflow. Villecrose (2001) showed the difficulty of comparing major avalanche situations when studying the main catastrophic crises in the French Alps. His study tries to define and to compare extreme situations by means of quantitative avalanche activity, damages, number of fatalities and depth of fresh snow. He concludes that those parameters are not enough and snow and weather context must be also included.

There are few works focused on the Pyrenees. An attempt to explain extreme avalanche events during the 1996 crisis by means of a synoptic approximation has been performed by Esteban et al. (2002, 2007). Classifications of synoptic patterns producing major avalanches in the Eastern Pyrenees have been proposed by García et al. (2007), but the study doesn't use any statistical method for clustering.

The purpose of this study is to contribute to better understand the occurrence of major avalanche episodes in the Eastern Pyrenees and their relation with atmospheric circulation patterns by means of statistical methods. First of all, we have tested whether major avalanches episodes might be considered rare events such as hail days or, for instance, snowing days at sea level in the Mediterranean climate context. Different statistical models have been applied to describe the observed distribution of major avalanches episodes in the Pyrenees. Second, multivariate statistical analyses have been used to determine which synoptic situations are

responsible for major avalanche episodes in the Eastern Pyrenees. As the final aim is to improve the regional avalanche warning, we consider that this method could be a helpful tool to reduce the high false alarm ratio when the regional forecasting of critical situations (levels High, 4, or Very High, 5) is based on expected new snow depth (Schweizer et al., 2008).

2. STUDY AREA

The Pyrenees constitute a mountainous system extending about 450 km from the Atlantic Ocean (west) to the Mediterranean Sea (east). They rise at the isthmus that links the Iberian Peninsula with the rest of the Euro Asiatic continent. The Eastern Pyrenees lie within the Spanish border and are 146 km long, with a width varying and varies from 19 km to 52 km and diminishing towards the east. Highest elevations reach 3,000 m, but at the study area elevation is mostly between 2,500 and 3,000 m. The timber line is located between 2,100 and 2,400 m approximately. The highest mountain villages are located up to an elevation of 1500 m. The highest winter opened roads reach 2,300 m and 9 alpine ski resorts are over 1,500 m altitude.

The Eastern Pyrenees is divided into 7 regions attending to the avalanche activity and snow conditions (figure 1). Avalanche coverture is shown by means of the shading, which corresponds to the area occupied by avalanche paths (Oller et al., 2006). These snow and avalanche regions are the empirical result of 15 years of avalanche forecasting since long term databases don't exist

Three climatic regions can be defined for the Eastern Pyrenees (García et al., 2007). The northwest part of the Eastern Pyrenees shows a humid ocean climate as the main river basin drains to the Atlantic Ocean through France. Precipitation is abundant and annual amounts don't vary strongly year to year. The total amount of fresh snow at 2200 m height is about 500-600 cm per year. Frequent and moderate snowfalls lead to high avalanche activity, and this area is where the maximum natural avalanche activity takes place. Precipitation linked to oceanic air masses diminishes quickly towards the south. So, in the intermountain region climate gains continental characteristics towards the south and east. Winter precipitation reduces being the winter the driest season and snow precipitation increases in the equinoctial seasons. Interannual variability of precipitation increases. The total amount of fresh snow at

2200 m height exceeds slightly 250 cm per year. Predominant winds come from north and northwest, often with gusts over 100 km/h. Snow cover depth is scarce, unstable structures persist on shadow slopes and wind slabs are frequent. In the most eastern part of the Eastern Pyrenees oceanic influence disappears completely and the Mediterranean Sea influence plays a significant role, resulting in heavy, but infrequent snowfalls, due to lows centred on the Mediterranean Sea blowing very humid, maritime flow from the east. Interannual variability of snowfalls is very high. The total amount of fresh snow at 2200 m height is about 350-450 cm per year. Predominant winds come from north (*mistral* or locally *tramuntana)* and maximum gusts sometimes exceed 200 km/h at 2200 m height due to the formation of a persistent low in the lee-side of the Alps over the Lion Gulf. Snow pack distribution is scarce and it often coexists with nude terrain above timber line due to the persistent wind. Hard slabs on lee sides are frequent.

Seven nivoclimatic regions are defined attending to different behaviour of the snowcover and avalanche activity. These differences in the conditions of the snowcover and avalanche activity are due to characteristics of the terrain (Oller et al., 2006), mainly, average elevation and aspect of the avalanche paths. These seven regions of the Eastern Pyrenees at the Spanish face are, from west to east: *Aran-Northern border of Pallaresa (AP)* with oceanic conditions; *Ribagorçana-Vall Fosca (RF)*, *Pallaresa (PL)*, *Perafita-Puigpedrós (PP)*, *Cadí Moixeró (CM)* with intermountain conditions; *Pre-Pyrenees (PR)* and *Ter-Freser (TF*) with Mediterranean influence. The regions are used to define specific warning avalanche bulletins.

3. DATA AND METHODOLOGY

A major avalanche episode is defined as the occurrence interval of time (minimum one day is considered) of at least one major avalanche registered. Episodes of exclusively major avalanches triggered by explosives have been rejected. We have considered major avalanches in a wide sense, as defined by Schaerer (1986), avalanches larger than usual, arriving to the bottom of the valley, destroying mature forest or damaging structures. All avalanches travelled further than 1000 m from the starting zone to the run out zone.

The main drawback is the lack of meteorological and avalanche observations in high-mountain in the Eastern Pyrenees, before the avalanche surveying and warning began in 1989. This is why an essential part of this work is to look for major avalanche events in the past, it means, dating and localizing. Hence, a research project called ALUDEX, founded by the Spanish Ministry of Technology and Education was the basis for identifying and dating evidence from past avalanche events by means of the morphology of the rings and damages in the timber (Muntán et al., 2004). In this way, some avalanches episodes at annual resolution and their spatial extent were identified in the Eastern Pyrenees.

In addition to annual resolution, major avalanches have been systematically dated at a daily resolution from 1996 until present. In 1996 the Nivometeorological Observers Network (NIVOBS) of the Geological Institute of Catalonia begun a winter surveillance making transects every day to report snow conditions and avalanche events. All the episodes have been dated and mapped by systematic observations in all seven regions by means of helicopter flights. Monthly or weekly resolution on avalanche dating exists from 1986 to 1996. Before 1986, avalanche dating is scarce and without continuity and data comes from enquiries to inhabitants; annual and monthly resolution prevails.

Major avalanches episodes are counted (N = 39) from 1970-71 to 2007-08 winter seasons (38 winters). In order to find out which of the theoretical probability distribution fits major avalanche episode occurrence, we used the Kolmogorov-Smirnov test with critical values of the Lilliefors test, at the 0,05 level of significance, to investigate whether the Poisson or the negative binomial distribution are adequate for the occurrence of annual major avalanches episodes. The Poisson distribution is used for rare events. In Statistics these events are those that have a low probability or are unlikely to occur. The probability function for the Poisson distribution is given by:

$$f(x) = \lambda^x \frac{e^{-\lambda}}{x!} \qquad (1)$$

where λ is the population mean and x is the number of events.

The negative binomial probability function is more suitable for most likely events which show a certain dependency among them to occur. The negative binomial probability function is given by:

$$f(x) = \frac{\Gamma(x+k)}{\Gamma(x+1)\Gamma(k)} \cdot \frac{p^x}{(1+p)^{k+x}} \quad (2)$$

where x is the number of events at year, and k and p are the parameters of the distribution.

Regarding circulation patterns that lead to major avalanches episodes, daily atmospheric circulation data at synoptic scale have been selected from the NCEP-NCAR reanalysis data (Kalnay at al., 1996) by using maps of 500 hPa geopotential height. This atmospheric level involves a strong time inertial component, which usually concatenates certain weather regimes well-known at surface level in the Pyrenees (Romero et al., 1999; Esteban et al., 2005). The obtained series of geopotential height values in meters (gpm) at 500 hPa topography comprise from 1970-71 to 2006-07 winter seasons (December to March). The grid ranges from 70º to 30º latitude N and from 30ºW to 20ºE longitude with a spatial resolution of 2,5º x 2,5º, that defines the North Atlantic-Western Europe zone. The lack of daily meteorological database recorded on the ground in high-mountain lead us to decide to analyse the 500 hPa geopotential height maps for the position of troughs and ridges, general flows, cut-off lows, dynamics and thermal anticyclones, which control the weather at synoptic scale and affects the evolution of the snow cover.

We used principal-component analysis (PCA) in the T-mode data matrix in order to relate circulation patterns and major avalanche episodes. This mode is the temporal mode (time-dependent) where the variables (columns) are the dates and the cases (rows) are the grid points. The values consisted of geopotential height values in meters (gpm) at 500 hPa during the winter seasons from 1970-71 to 2006-07 from 357 grid points. The definitive number of components was decided by means of the explained variance criteria and the Scree test (Cattell, 1966). The next step was to perform an orthogonal rotation of the components by the Varimax method to allow in interpretability of the low-variance principal components and in raising their weights. One new component is obtained by a negative correlation respect to the

data set of another component (component 4); next, the grid cells of the different avalanching days that would integrate this hypothetic new component has been put to the parametric ANOVA test which has confirmed no significant statistical differences between those cases; so they are put into in the same component which is called 6.

Next, we consider the relationship between the atmospheric circulation patterns leading extreme avalanches and the average atmospheric conditions. Hence, we have mapped the anomalies of the geopotential heights (in meters) at which the pressure value of 500 hPa is attained for each principal component respect to the average 500 hPa heights in geopotential meters distribution for the winter seasons corresponding to the 1970-71 to 2006-07 data. This operation consists of subtracting the standardized values of the average 500 hPa geopotential height values of each component representing all the major avalanche episodes from the daily average of the 1970-71 to 2006-07 period, previously extracting the avalanche episodes dates. So, the maps are obtained from the arithmetic differences between the average 500 hPa heights in geopotential meters of each point of the grid of each component respect to the average 500 hPa geopotential height for the period 1970-71 to 2006-07, divided by the standard deviation of the last data set. The maps represent the variable meters after having been converted in a standardised variable. The anomaly maps give an idea of the role that the North Atlantic Oscillation index (NAOi) plays in the occurrence of extreme avalanche episodes in the Eastern Pyrenees. The NAO, as a low frequency circulation pattern, determines strongly the variability of the temperature and precipitation behaviour in Europe (Hurrel, 1995; Beniston et al., 1996). The interest of connecting extreme avalanche episodes with NAOi lies in the fact of NAOi for the next winter seems to be predictable at medium term with a reasonable level of confidence (Jones et al., 1997).

4. RESULTS AND ANALYSES

Results in figure 2 show that the annual probability of recording at least one extreme avalanche episode in the Eastern Pyrenees is 64% according to the Poisson model and 62% according to the negative binomial model. Maximum absolute value of differences between observed and calculated accumulate frequencies is 0.069 for Poisson and 0.087 for negative

binomial. Hence, the best fit with the Kolmogorov-Smirnov test and Lilliefors critical values at the 0.05 level of significance corresponds to the Poisson distribution (0.073) while for the negative binomial was of 0.055.

Results in table 1 show that there is a larger probability to register at least one major avalanche episode than no one. Major snow avalanche in the Eastern Pyrenees is a rare natural event but not exceptional. The maximum observed major avalanche activity took place in the winter 1995-96 when 6 episodes were registered and 144 large avalanches were mapped.

The annual frequency of major avalanches episodes obtained by fitting varies widely from one region to another in Eastern Pyrenees, despite the fact that they are very similar in latitude and distance (table 2). The region of oceanic climate (*Aran-Northern border of Pallars*, *AR*) shows the highest probability of suffering at least one episode at year (44%). The probability diminishes drastically to the eastern, towards intermountain climate regions where the calculated probability of having at least one annual episode is less than 15% (*Perafita-Puigpedrós*, *PP*; *Cadí-Moixeró*, *CM*). Major avalanches could be considered an exceptional natural event in the region *Perafita-Puigpedros* (*PP*), where an annual probability of 3% is expected. In this case, geographic factors play a very important role since this range is sheltered from humid flows. This area is a pluviometric shadow where vegetation is clearly xerophile. Moving towards the east, close to Mediterranean Sea, the annual probability of at least one annual extreme avalanche episode increases again to 25% (*Ter-Freser, TF*), linked probably to cyclogenetic processes characteristic of Western Mediterranean Sea.

The broad regional variability observed in major avalanche activity implies spatial variations in the relationship between major avalanche episodes and synoptic patterns. Applying PCA to the days with major avalanche activity, major avalanche episodes are gathered in six principal components, which explain the 94% of the total variance of the sample.

The interpretation of each component is based on observed data, not simulated data. The first component, representing the 39% of the total variance, identifies northern and north-western advections over the Eastern Pyrenees (figure 3). It explains 12 major avalanche episodes from 1970/71 to 2006/07. Generally, the Azores high pressures are extended over the Atlantic Ocean, while a deep low pressure is located on the axis Baltic Sea-Italian Peninsula.

This configuration pumps either an artic or a maritime polar air mass over the Pyrenees. This pattern generates very low temperatures (-15º to -20ºC at 2200 m height), intense snowfalls, strong winds and very active drift snow processes. A snowfall about 100-150 cm in 24 hours were recorded at *Aran-Northern border of Pallars* (January 2003). Major powder avalanches are frequent, but restricted to this region. Sometimes, wet snow avalanches release due to the pass of a warm front few days after a cold front had crossed. Precipitation gradient decreases strongly towards the south and east. In the rest of the regions, major slab avalanches prevail specially located in southern slopes due to the enormous overloading of drifted snow deposited on lee side aspects, but exclusively if fresh snow previously exists on the ground. This was the case of 6th February of 1996, when many exceptional slab avalanches affected the *Ter-Freser* region; timber analysis of trees killed by the avalanches indicated ages about 80 years old in the middle of one avalanche path in *Ter-Freser*, even 200 years old in the distal flanks.

The components 2 and 3 gather together a 31% of the total variance, sharing a similar weight. These components are the main atmospheric patterns producing major avalanche episodes in the most eastern regions of the study site (*Prepirineu and Ter-Freser*), the area of Mediterranean influence.

Component 2 explains 4 major avalanche episodes from 1970/71 to 2006/07. This component is characterized by a long trough at 500 hPa exhibiting an oblique axis oriented NW-SE, due to the Siberian high over Europe which diverts troughs to the Mediterranean basin (figure 4). Normally, it yields a small low at surface level in front of the Eastern coast. Humid, maritime flow on surface produces heavy precipitations in the closest regions to the Mediterranean Sea. Instability is high due to the contrast between cold air at 500 hPa and relatively warm air mass at low levels. The snowpack usually contains weak layers with depth hoar and faceted grains before fresh snow arrives, since low temperatures and strong irradiation has prevailed below the Siberian high pressures influence. So, avalanche activity is favoured due to the surcharge of new fallen snow.

Component 3 is explained by a blocking high pressures situation at 500 hPa over Central and North-Western Europe and a cut-off low centred over the south of the Iberian Peninsula-North of Africa (figure 5). It explains 4 major avalanche episodes in the studied period. In this component, we want to focus on the mesoescalar observed meteorological

phenomena with strong consequences in avalanche dynamics. Comparing conditions to those related to component 2, we observed that component 3 is related with high pressures (1015-1020 hPa) on the surface level all over the Pyrenees, but cyclonic circulation rules on upper levels. Also, a warm and very humid Mediterranean flow on surface penetrates from the east affecting the regions closest to the Mediterranean Sea, even also at region as distant as *Ribagorçana-Vallfosca*, which is well-faced south. In one case included in the component 3 a sum of precipitation of about 400 mm (SWE) was recorded during four days in regions of mediterranean influence in December 1991, with snow level around 1800-2000 m height. Exceptional avalanches of wet, loose snow were released in *Ter-Freser*, the nearest region to Mediterranean Sea. Eastern advection is a synoptic pattern integrated in the component 3 and observed usually in September-October giving torrential precipitations in coastal mountain ranges but seldom in winter (Jansà, 1990).

Components 4, 5 and 6 account for the remaining 24% of the total variance. Component 4 is defined by a deep low with a very cold core at 500 hPa over the Lion Gulf (figure 6). It also reflects a deep low on surface levels. Northern, strong winds and heavy snowfalls affect not only Pyrenees but also the coastal line. Major powder avalanches were registered in disparate regions. Only one major avalanche episode is explained by this component. For component 5, a wide low pressure is located at high and low levels in the west of the Iberian Peninsula (figure 7). From surface to upper levels south and south-western winds flow carrying warm and humid air from Atlantic and even Mediterranean on lower levels over the Pyrenees. This component explains 2 major avalanche episodes. The most intense major avalanche episode occurred at the end of 1996 January due to a south-western advection situation. Many major avalanches of fresh, humid and dense snow felt down few hours after the precipitation. Four regions were affected by major avalanches. A maximum snowfall of 220 mm of snow water equivalent (SWE) in 24 hours was registered in Port del Comte (*Pre-Pyrenees*) on 22th January 1996 and many other exceeding 150 mm of SWE in several regions due to processes of convective cells growth. This precipitation corresponds to a recurrence period that exceeds 100 years (Gumbel estimation). As Esteban et al. (2005) have shown, very intense precipitation affects the southern side of the Pyrenees in such synoptic circulation pattern. Nevertheless, snow is registered only in the highest elevations, normally over 2200 m height.

Finally, component 6 is linked to avalanches triggered by major melting episodes. That is why a ridge from the subtropical anticyclonic belt spreads further north over the Western Mediterranean Sea (figure 8). Usually a warm advection at low levels (850, 700 hPa) gets right into the Pyrenees. Snow cover suffers melting processes suddenly and major avalanches have fallen when the inner layers still contained cold, persistent grains such us depth hoar and facets. This component has been observed to precede major avalanches in late March after cold winters. It explains 2 major avalanche episodes from 1970/71 to 2006/07. All events are wet snow avalanches.

In order to know the normality of the obtained synoptic patterns it seems interesting to compare them to the average winter atmospheric circulation. We have also considered putting them in relation to the North Atlantic Oscillation index (NAOi). A monthly NAO index is calculated from the normalized pressure difference between Reykjavik and Gibraltar from December to March. Data was obtained from Jones et al. (1997). Positive values indicate zonal, westerly atmospheric circulation where low pressures are located over the North Atlantic and high pressures over Azores Islands. In the opposite case, for negative values, low pressures circulate more towards south than usual due to a weakening of the Azores high pressures and vortexes cross the Iberian Peninsula. In some mountain ranges of Europe as the Alps the evolution of the main meteorological parameters as temperature, precipitation and winds are conditioned by the NAOi (Beniston, 1996). At the Pyrenees, the investigations on the relationship between winter precipitation and NAOi show a negative correlation (Martín-Vide et al., 1999; Esteban et al., 2001) for many regions.

The relationship between NAOi and snow avalanche release has been analyzed for different regions in Europe by Keylock (2002) in Iceland and Jamelli et al. (2007) in the French Alps. Rank correlations between the NAOi (December-March) and the number of major avalanche episodes in the Eastern Pyrenees are significant at the 5% level with values of -0,45 for the period 1970-71 to 2005-06 and -0,63 for the period 1988-89 to 2005-06, when data are systematically registered. Keylock (2002) proposes a new NAO index that cumulates consecutive positive values of NAOi monthly since he demonstrates that this new index is a better predictor of avalanching in Iceland than the actual definition of NAOi. As correlation between avalanche episodes per year and NAOi is negative in the Eastern Pyrenees (R = -0.45

for 1970/71 to 2005-06 and R = -0.63 for 1988/89 to 2005-06 when observations are systemathic), a cumulative negative of NAOi is applied (CNI). From 144 months to December-March for the period 1970-71 to 2005-06, 92 months have cumulative positive NAO index and 52 a negative index. An overall of 22 avalanche episodes are registered; 13 occurred with negative index and 9 with positive index. Of the 13 avalanche episodes with a negative index, 9 avalanche episodes were recorded with a maximum CNI value less than -4.0. Of 173 avalanche events observed during negative CNI values, 159 of these are registered with a maximum CNI value less than -5.0 (average value for negative CNI months = -2.3 and median value = -1.9). Rank correlation between the CNI and avalanche episodes per year (R = -0.83) is higher than equivalent correlation for the NAO. From these preliminary overlook, it seems to be that number of episodes and number of events per episode increases when negative CNI reaches relatively low values.

Once values of pressure for each component have been subtracted from the average pressure values (1970-2007), we elaborate seven composite-anomaly maps with standardized values. These composite-anomaly maps represent the deviation of the 500 hPa heights in geopotential meters of each component respect to the mean atmospheric circulation, this is, how strongly a component is expressed relative to the average climatology. (11) Indirectly, the spatial distribution of the positive and negative anomalies over the map shows in a visual way the relation of that component respect to the NAOi, In this way, when one component map shows both negative anomalies over the south-western Atlantic Ocean and positive anomalies over the north Atlantic Ocean it means that it is associated to a negative phase of NAO and vice versa. The composite-anomaly map of component 1 shows the minimum anomalies with respect to the average atmospheric circulation and it can be considered as a relatively frequent weather situation (figure 9). It is linked to positive and neutral NAOi. Its spatial extent in terms of major avalanche releasing is the widest, affecting all the regions, but mainly *Aran-Northern border of Pallars* (AR), 34% of the cases (table 3). The composite-anomaly map of component 2 is defined by a high negative anomaly in the pressure distribution over the Iberian Peninsula (figure 10). The composite-anomaly map of component 3 diverges markedly from the average synoptic conditions (figure 11), resulting in an average anomaly of 1.0 absolute value for each grid point. The component 4 shows an exceptional anomaly over the Eastern Pyrenees (figure

12). The component 5 exhibits the maximum anomaly at 500 hPa (figure 13) in absolute values for the all grid (average of 1.3). The component 6 is the only component reflecting pressures at 500 hPa higher than usual over the Pyrenees (figure 14). In table 4 main characteristics of the major avalanche episodes and the percentage of variation attributable to each components are shown.

5. DISCUSSION AND CONCLUSIONS

This contribution has studied major avalanches activity without the presence of a long-term snow-climatic database. Results highlight that large regional differences exist in major avalanche activity. These differences are detected both in the occurrence of major avalanche episodes and in the spatial extent of each atmospheric component yielding major avalanche activity (figure 15). We have recourse to annual resolution by inquiring into dendro-geomorphological method and found out daily dating in historical documentation. Daily avalanche dating is provided also from systematic population enquiries. Thanks to this diverse approach, for the first time values statistically significant of occurrence probability of major avalanches activity is furnished at regional scale for the Spanish Eastern Pyrenees. It should promote and reinforce planning actions in forecasting and zonation the avalanche hazard in Spain.

Dating major avalanches episodes has allowed a classification of related synoptic patterns by means of PCA, which should improve the avalanche warnings. Comparing atmospheric patterns giving major avalanches with atmospheric patterns leading heavy snowfalls in the Eastern Pyrenees, differences are found. Esteban et al. (2005) propose seven atmospheric circulation patterns related to heavy snowfall days with an intensity of at least 30 cm of snow in a period of 24 hours in Andorra (Eastern Pyrenees). Our classification does not include any atmospheric pattern concerning zonal flows from the west which are responsible of intense snowfalls detected in the Esteban's classification. The reason for differences in avalanche activity for critical new snow amounts probably falls on both the profile storm and the previous snowpack stability. Mainly, evolution of temperature, wind and intensity of the snowfall during the storm should be considered to explain differences in the effectiveness of critical snow

amounts. Future work might focus on characterising the storm profile for each synoptic pattern and the behaviour of the most significant variables that affect the snowpack conditions. Also, our atmospheric patterns classification provides for a major avalanche situation not linked to heavy snowfalls but melting processes. In some occasion mesoescalar phenomena have had a main role in the avalanche releasing, especially in components linked to Mediterranean ciclogenesis. In these cases, synoptic scale would not be the unique approach to define components completely.

We also endeavour to look for the relations between atmospheric patterns giving avalanches and atmospheric low-frequency patterns that indicate weather trends at medium-term, as NAO for the Pyrenees. The 500 hPa composite-anomaly maps of the principal components leading major avalanches likely suggest more probable major avalanche episodes for negative phase of NAO, since components 2, 3, 4 and 5 occurs when positive anomalies are detected over Iceland and negative over Gibraltar (South of the Iberian Peninsula). These components gather the most part of the total explained variance. It's interesting to note that the 1995-96 winter season, the maximum in major avalanches activity, broke the record of NAOi negative anomaly (-2.35) from 1970 till 2008. There is a negative correlation between NAOi and major avalanches releasing in the Eastern Pyrenees, which is higher by applying a cumulative NAO index. In a broader geographical context, this issue is remarkable since connections have been found in areas close to the centres of the NAO dipole as Iceland, but not in further areas as the French Alps.

Finally, in spite of being a small geographical area compared to the Rocky Mountains or the Alps, results in occurrence probability of major avalanche episodes and extent of atmospheric patterns reflect also a significant spatial variability at regional scale, which must be taken into account when applying protection and prevention strategies. Geographical and climatic factors account for this spatial variability. Among the geographical factors, the zonal alignment of the axial range lets the retention of humid air masses, both polar and artic from north advections, and tropical air masses from south and southwest flows. The meridian valleys configuration favours the penetration and the placement of the unstable air masses pointed out; the forced lifts by the relief sometimes result on heavy and persistent snowfalls, even stationary convective cells. The proximity to Mediterranean Sea and less to the Atlantic Ocean avoids

extreme temperatures as it occurs in inland ranges but surprisingly extensive precipitation shadows exist as well. Among the climatic factors, the relatively low latitude of the massif becomes the Pyrenees in an oscillating boundary between the humid ocean climate due to dynamic lows and dry climate associated to subtropical semi-permanent anticyclone belt. In abstract, relieve and marginal position with respect to the main climatic action centres (Atlantic lows and subtropical high pressures) explain why some components have local effects. The challenge is making progress in the accurate identification of the snow structure and stability conditions to assess the effectiveness of each atmospheric pattern associated to major avalanches.

To conclude, in a broader climatic context, the preliminary results of the connection between avalanching and NAO in the Eastern Pyrenees open a investigation line to be explored in greater depth.

ACKNOWLEDGEMENTS

Dendrochronological contribution comes from the Project ALUDEX (MICYT-FEDER: REN2002-02768), executed with the financial support from the Spanish Ministry of Technology and Education, project REN2002-02768/RIES, the European funding agency FEDER and the Autonomous Organism of National Parks from the Environmental Ministry, project 11/2003. Project ALUDEX was collaboration between the Cartographic Institute of Catalonia, the University of Barcelona, the Meteorological Survey of Catalonia and the General Council of Aran. Project REN2002-02768/RIES was collaboration between Geological Institute of Catalonia and the University of Barcelona. We are grateful to Aline Concha for reviewing the English version and Santi Manguan for his technical support. We want also to thank two anonymous reviewers for providing many useful comments.

REFERENCES

Armstrong, R.L. and Armstrong, B.R., 1987. Snow and avalanche climates of the western United States: a comparison of maritime, intermountain and continental conditions. International Association of Hydrological sciences Publication, 162: 281-294.

Beniston, M. and Rebetez, M., 1996. Regional behaviour of minimum temperatures in Switzerland for the period 1979-1993. Theor. Appl. Climatol., 53, Springer-Verlag: 231-243.

Birkeland, K.W., Mock, C.J. and Shinker, J.J., 2001. Avalanche extremes and atmospheric circulation patterns. Annals of Glaciology, 32: 135-140.

Cattell, R.B., 1966. The scree test for the number of factor. Multivariate Behav. Res, 1: 245-276

Eckert, N., Parent, E., Naaim, N. and Richard, D., 2007. Bayesian stochastic modelling for avalanche predetermination: from a general system framework to return period computations. Stochastic Environmental Research and Risk Assesment, 22. 2: 185-206.

Esteban, P., Soler, X., Prohom, M. and Planchon, O., 2001. La distribución de la precipitación a través del índice NAO. El efecto del relieve a escala local: El Pirineo Oriental. In: J.A. Guijarro Pastor, M. Grimalt Gelabert, M. Laita Ruiz de Asúa y S. Alonso Oroza (Eds.), El Agua y el Clima - L'Aigua i el Clima. Publications of the Spanish association of climatology (AEC), 2002, Serie A, nº 3. Planográfica Balear, Marratxí (Mallorca), pp. xii+594.

Esteban, P., Mases, M. and Martin-Vide, J., 2002. Climatologia per a la predicció d´allaus: l´allau de Les Fonts d´Arinsal, Andorra, 8 de febrero de 1996. Horitzó 2: 10-19.

Esteban, P., Jones, P.D., Martín-Vide, J. and Mases, M., 2005. Atmospheric circulation patterns related to heavy snowfall days in Andorra, Pyrenees. International Journal of Climatology 25: 319-329.

Esteban, P., Martí, G., García, C., Aran, M., García, A., Gavaldà, J. and Moner, I., 2007. Heavy snowfalls and avalanche activity over Eastern Pyrenees: a study of two extreme cases. Proceedings of the Alpine&Snow Workshop, 44-48.

Fitzharris, B.B., 1981. Frequency and Climatology of Major Avalanches at Roger Pass, 1909-1977. National Research Council, Canadian Association Comittee on Geotechnical Research, Ottawa, 99.

García, C., Martí, G., García, A., Muntán, E., Oller, P., and Esteban, P., 2007. Weather and snow pack conditions of major avalanches in the Eastern Pyrenees. Proceedings of the Alpine&Snow Workshop, 49-56.

Hächler, P., 1987. Analysis of the weather situations leading to severe and extraordinary avalanche situations. International Association of Hydrological Sciences Publication, 162: 295-303.

Hewit, K., 1970. Probabilistic approaches to discrete natural events: a review and theoretical discussion. Clark University.

Hurrell, J.W., 1995. Decadal trends in the North Atlantic Oscillation and relationships to regional temperature and precipitation. Science 269, 676-679.

Jansà, A., 1990. Notas sobre análisis meteorológico mesoescalar en niveles bajos. Instituto Nacional de Meteorología. Madrid.

Jomelli, V., Delval, C., Grancher, D., Escande, S., Brunstein, D., Hetu, B., Filion, L. and Pech, P., 2007. Probabilistic analysis of recent snow avalanche activity and weather in the French Alps. Cold Regions Science and Technology, Vol. 47: 180-192.

Jones, P.D., Jonsson, T., and Wheeler, D., 1997. Extension to the North Atlantic Oscillation using early instrumental pressure observations from Gibraltar and South-West Iceland. Int. J. Climatol. 17: 1433-1450.

Kalnay, E., Kanamitsu, M., Kistler, R., Collins, W., Deaven, D., Gandin, L., Iredell, M., Saha, S., White, G., Woollen, J., Zhu, Y., Chelliah, M., Ebisuzaki, W., Higgins, W., Janowiak, J., Mo, C.K., Ropelewski, C., Wang, J., Leetma, A., Reynolds, R., Jeene, R. and Joseph, D., 1996. The NCEP/NCAR 40 years reanalysis project. Bulletin of the AMS, 77: 437-471.

Keylock, C.J.,2003. The North Atlantic Oscillation and snow avalanching in Iceland. Geophys. Res. Lett., Vol.30. Nº5 (58): 1-4.

LaChapelle, E.R. 1966. Avalanche forecasting. A modern synthesis. International Association of Hydrological Sciences Publication. Vol. 69. 350-356.

Martín-Vide, J; Barriendos, M.; Peña, JC.; Llasat, MC. and Rodríguez, R., 1999. Potencialidad del índice NAO en la previsión de episodios de alta pluviometría en España. Análisis, GR 67: 19-29.

Martínez, P. and Oller, P., 2004. Accidents per allaus a Catalunya. I Jornades Tècniques de Neu i Allaus. Institut Cartogràfic de Catalunya, Barcelona, Spain, pp. 4.

McClung, D.M., 2000. Extreme avalanche runout in space and time. Canadian Geotechnical Journal. J. 37(1): 161-170.

Mock, C.J., 1996. Avalanche Climatology of Alyeska, Alaska, U.S.A. Arct. Alp. Res., 28(4), 502-508.

Muntán, E., Andreu, L., Oller, P., Gutiérrez, E., and Martínez, P., 2004. Dendrochronological study of the avalanche path Canal del Roc Roig. First results of the ALUDEX project in the Pyrenees. Annals of Glaciology, 38: 173-179.

Oller, P., Muntán, E., Marturià, J., García, C., García, A., Martínez, P., 2006. The avalanche data in the Eastern Pyrenees. 20 years of avalanche mapping. Proceedings of the ISSW. Telluride, Colorado, USA, pp. 305-313.

Osborn, T.J., Briffa, K.R., Tett, S.F.B., Jones, P.D. and Trigo, R.M., 1999. Evaluation of the North Atlantic Oscillation as simulated by a coupled climate model. Climate Dynamics, 15: 685-702.

Romero, R., Sumner, G., Ramis, C., Genovés, A., 1999. A classification of the atmospheric circulation patterns producing significant daily rainfall in the Spanish Mediterranean area. International Journal of Climatology, 19: 765-785.

Sakamoto, C. M., 1973. Application of the Poisson and negative binomial models to thunderstorm and hail days probabilities in Nevada. Monthly Weather Review, Vol 101, nº 4: 350-355.

Schaerer, P., 1986. Weather patterns for major avalanches. The avalanche Review, vol. 4, nº 3: 2.

Schweizer, J., Mitterer, C., Stoffel, L., 2008. Determining the critical new snow depth for a destructive avalanche considering the return period. Proceedings of International Snow Science Workshop, 292-298.

Thom, H., 1966. Some methods of climatological analysis. Technical Note Nº 81, WMO, Geneva, Switzerland, pp. 30-34.

Villecrose, J., 2001. Les avalanches de janvier et fevrier 1999 dans les Alpes du Nord Françaises. La Météorologie 8º série, 32: 11-22.

TABLES

Nº Episodes	fi	Obs. Prob.	Calc. Prob.	
			Poisson	Neg. Bin
0	11	0.289	0.358	0.376
1	19	0.500	0.368	0.351
2	7	0.184	0.189	0.179
3	0	0.000	0.065	0.067
4	0	0.000	0.017	0.020
5	0	0.000	0.003	0.005
6	1	0.026	0.001	0.001
7	0	0.000	0.000	0.000

Table 1. Observed and calculated annual probabilities for the quantity of major avalanches episodes in the Eastern Pyrenees (1970/71-2007/08) with Poisson and negative binomial models.

Nº	Regions						
Epis.	AR	RF	PL	PP	CM	PR	TF
0	0.560	0.692	0.789	0.974	0.854	0.900	0.749
1	0.324	0.255	0.187	0.026	0.135	0.095	0.217
2	0.094	0.047	0.022	0.000	0.011	0.005	0.031
3	0.018	0.006	0.002	0.000	0.001	0.000	0.003
4	0.003	0.001	0.000	0.000	0.000	0.000	0.000

Table 2. Calculated annual probabilities for the number of major avalanches episodes at the 7 regions of the study area (1970/71-2007/08).

Comp.	Regions							
	AR	RF	PL	PP	CM	PR	TF	Total
1	8	5	4	1	1	1	2	22
2	2	0	1	0	2	2	1	8
3	0	3	1	0	1	1	2	8
4	0	1	0	0	0	0	1	2
5	1	2	1	0	0	0	1	5
6	1	0	0	0	1	0	0	2
Total	12	11	7	1	5	4	7	47

Table 3. Regions affected for every component (one episode can affect more than one region).

Date	Affected region							Component Variation	Avalanche type
	AR	RF	PL	PP	CM	PR	TF		
1/17/1972	X		X		X		X	2 (16%)	---
10/30/1974	X	X						1 (39%)	---
1/12/1979		X	X					1	---
1/18/1979		X						5 (8%)	---
1/16/1981	X							1	Wet snow
1/31/1986		X					X	4 (10%)	Powder
12/2/1991		X					X	3 (15%)	
10/5/1992	X							1	Wet snow
2/10/1994	X							1	Wet snow
1/12/1995	X		X				X	1	Wet snow
1/22/1996	X	X	X				X	5	Powder
2/6/1996		X	X	X	X	X	X	1	Slab
2/22/1996		X						1	Slab
3/14/1996	X							2	---
3/22/1996							X	6 (6%)	Wet snow
1/10/1997		X						1	Slab
1/21/1997		X	X					3	Wet snow
12/18/1997						X		2	Slush
1/31/2003	X		X					1	Powder
2/27/2003					X	X		2	Loose snow
1/2/2004	X							1	Powder
1/21/2005	X							1	Loose snow
1/30/2006					X	X	X	3	Loose snow
3/26/2006	X				X			6	Wet snow
4/2/2007		X						3	Loose snow

Table 4. Main characteristics of the major avalanche episodes and percentage of variation for each component.

FIGURE CAPTIONS

Figure 1. The Eastern Pyrenees location. The area of study has been divided into seven nivoclimatic regions. Avalanche paths surface is also shown.

Figure 2. Comparison of the observed cumulative frequencies of annual extreme avalanches episodes with the theoretical probabilities of Poisson and negative binomial distributions in the Eastern Pyrenees (1970/71-2007/08).

Figure 3. Atmospheric circulation pattern corresponding to component 1. 500 hPa heights in geopotential meters (gpm) are shown.

Figure 4. Atmospheric circulation pattern corresponding to component 2. 500 hPa heights in geopotential meters (gpm) are shown.

Figure 5. Atmospheric circulation pattern corresponding to component 3. 500 hPa heights in geopotential meters (gpm) are shown.

Figure 6. Atmospheric circulation pattern corresponding to component 4. 500 hPa heights in geopotential meters (gpm) are shown.

Figure 7. Atmospheric circulation pattern corresponding to component 5. 500 hPa heights in geopotential meters (gpm) are shown.

Figure 8. Atmospheric circulation pattern corresponding to component 6. 500 hPa heights in geopotential meters (gpm) are shown.

Figure 9. Anomaly maps for 500 hPa heights in geopotential meters (gpm) corresponding to component 1 (standardized values), respect to average atmospheric conditions.

Figure 10. Anomaly maps for 500 hPa heights in geopotential meters (gpm) corresponding to component 2 (standardized values), respect to average atmospheric conditions.

Figure 11. Anomaly maps for 500 hPa heights in geopotential meters (gpm) corresponding to component 3 (standardized values), respect to average atmospheric conditions.

Figure 12. Anomaly maps for 500 hPa heights in geopotential meters (gpm) corresponding to component 4 (standardized values), respect to average atmospheric conditions.

Figure 13. Anomaly maps for 500 hPa heights in geopotential meters (gpm) corresponding to component 5 (standardized values), respect to average atmospheric conditions.

Figure 14. Anomaly maps for 500 hPa heights in geopotential meters (gpm) corresponding to component 6 (standardized values), respect to average atmospheric conditions.

Figure 15. Frequencies of each component that lead major avalanches at oceanic, intermountain and Mediterranean areas.

FIGURES COLOUR

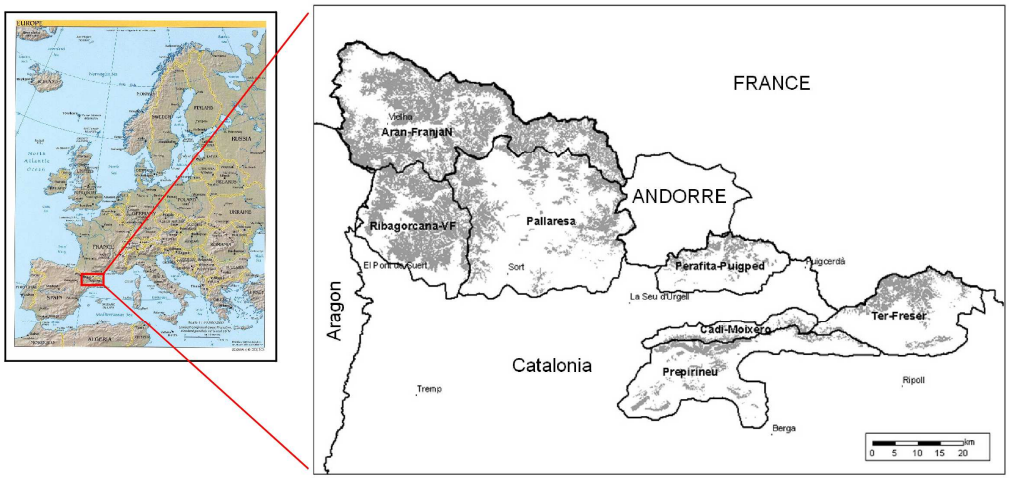

Figure 1

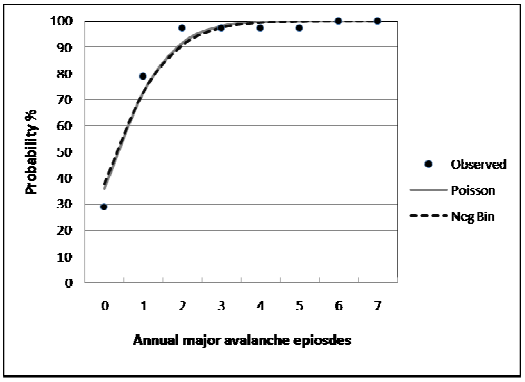
100
90
80
70
60
50
40
30
20
10
0
Probability %
0
1
2
3
4
5
6
7
Annual major avalanche episodes
Observed
Poisson
Neg Bin

Figure 2

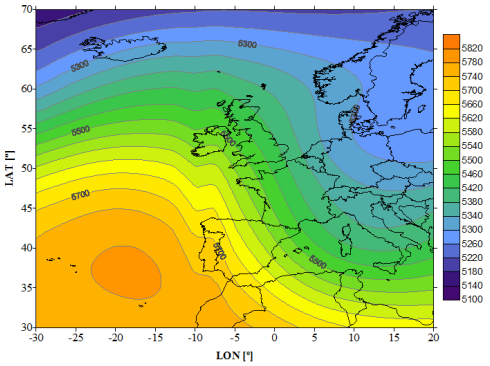
LAT [°]
LON [°]
5300
5500
5700
5900
6100
5820
5780
5740
5700
5660
5620
5580
5540
5500
5460
5420
5380
5340
5300
5260
5220
5180
5140
5100

Figure 3

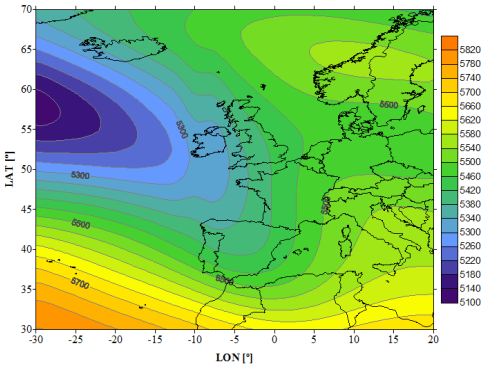
LAT [°]
LON [°]
5820
5780
5740
5700
5660
5620
5580
5540
5500
5460
5420
5380
5340
5300
5260
5220
5180
5140
5100

Figure 4

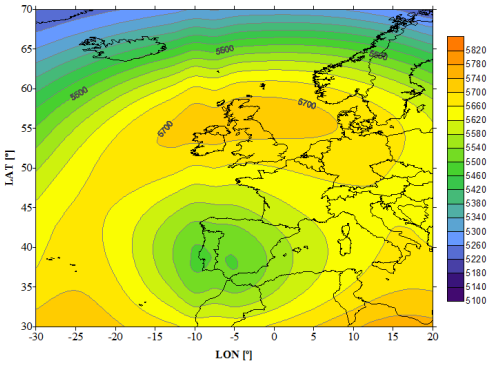
LAT [°]
LON [°]
5820
5780
5740
5700
5660
5620
5580
5540
5500
5460
5420
5380
5340
5300
5260
5220
5180
5140
5100

Figure 5

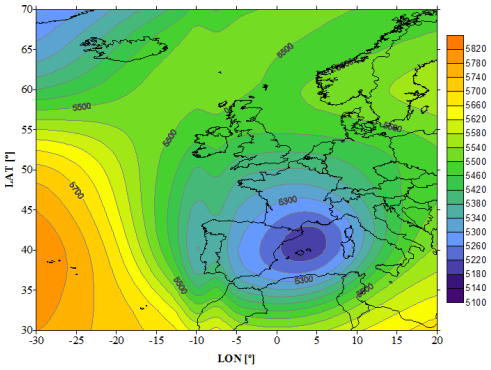
LAT [°]
LON [°]
5820
5780
5740
5700
5660
5620
5580
5540
5500
5460
5420
5380
5340
5300
5260
5220
5180
5140
5100

Figure 6

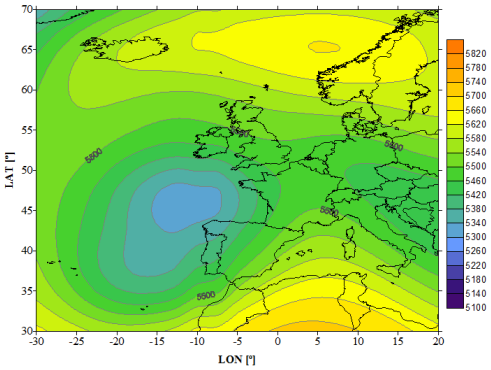
LAT [°]
LON [°]
5820
5780
5740
5700
5660
5620
5580
5540
5500
5460
5420
5380
5340
5300
5260
5220
5180
5140
5100

Figure 7

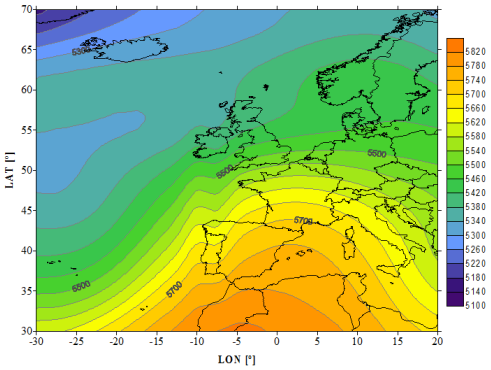
LAT [°]
LON [°]
5820
5780
5740
5700
5660
5620
5580
5540
5500
5460
5420
5380
5340
5300
5260
5220
5180
5140
5100

Figure 8

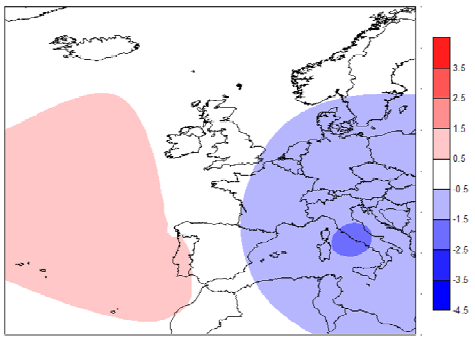

Figure 9

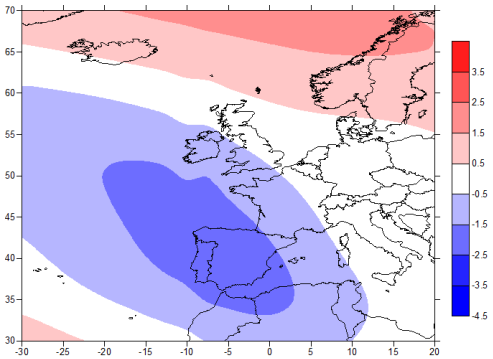
70
65
60
55
50
45
40
35
30
-30
-25
-20
-15
-10
-5
0
5
10
15
20
3.5
2.5
1.5
0.5
-0.5
-1.5
-2.5
-3.5
-4.5

Figure 10

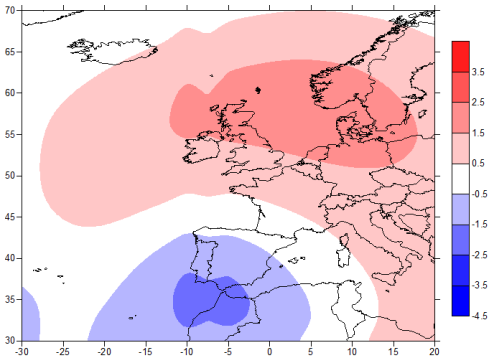
70
65
60
55
50
45
40
35
30
-30
-25
-20
-15
-10
-5
0
5
10
15
20
3.5
2.5
1.5
0.5
-0.5
-1.5
-2.5
-3.5
-4.5

Figure 11

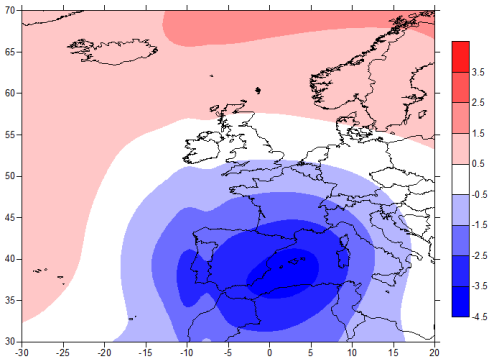
70
65
60
55
50
45
40
35
30
-30
-25
-20
-15
-10
-5
0
5
10
15
20
3.5
2.5
1.5
0.5
-0.5
-1.5
-2.5
-3.5
-4.5

Figure 12

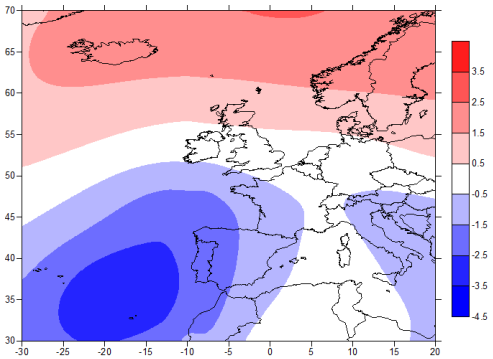
70
65
60
55
50
45
40
35
30
-30
-25
-20
-15
-10
-5
0
5
10
15
20
3.5
2.5
1.5
0.5
-0.5
-1.5
-2.5
-3.5
-4.5

Figure 13

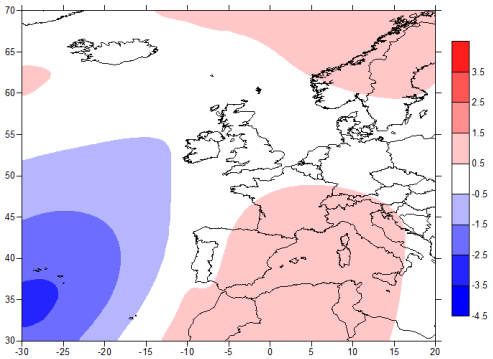
70
65
60
55
50
45
40
35
30
-30
-25
-20
-15
-10
-5
0
5
10
15
20
3.5
2.5
1.5
0.5
-0.5
-1.5
-2.5
-3.5
-4.5

Figure 14

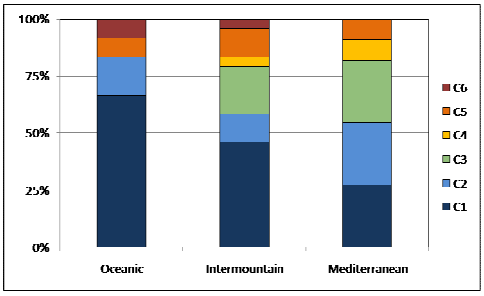
100%
75%
50%
25%
0%
Oceanic
Intermountain
Mediterranean
C6
C5
C4
C3
C2
C1

Figure 15

FIGURES BLACK & WHITE

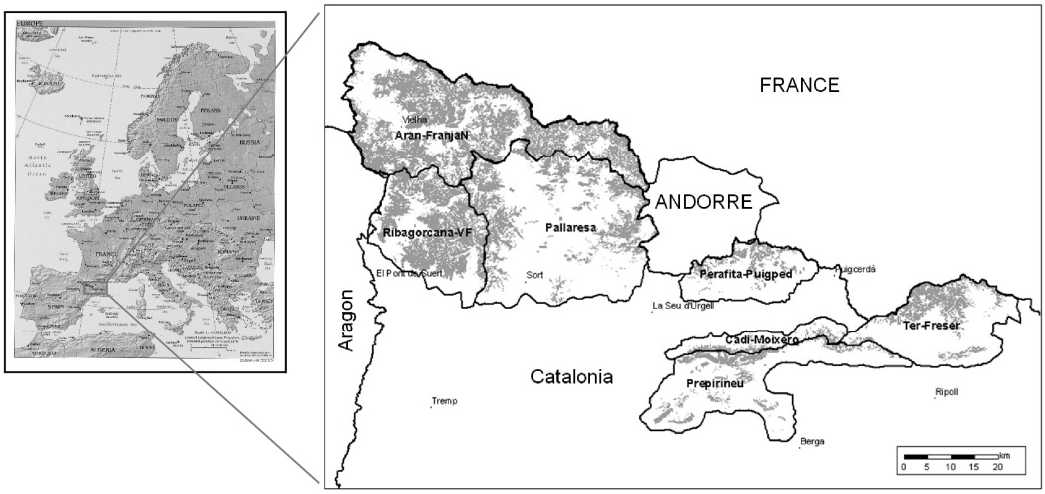

Figure 1

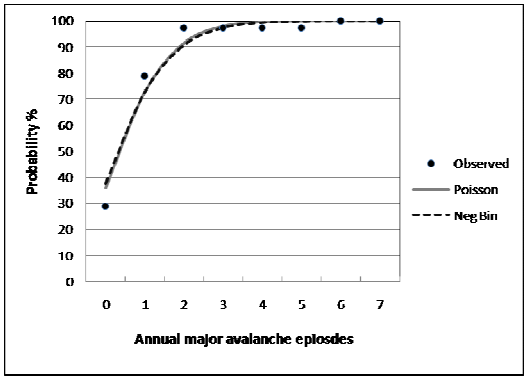
100
90
80
70
60
50
40
30
20
10
0
Probability %
0
1
2
3
4
5
6
7
Annual major avalanche eplosdes
Observed
Poisson
Neg Bin

Figure 2

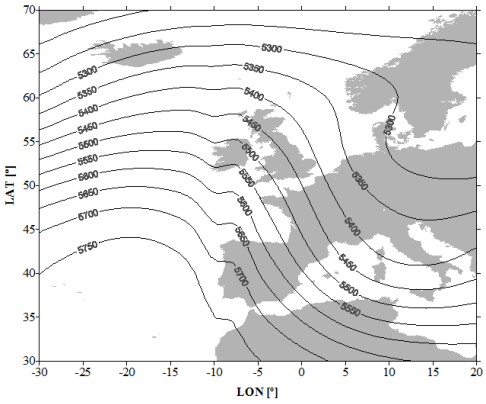
LAT [°]
LON [°]
70
65
60
55
50
45
40
35
30
-30
-25
-20
-15
-10
-5
0
5
10
15
20
5300
5350
5400
5450
5500
5550
5600
5650
5700
5750

Figure 3

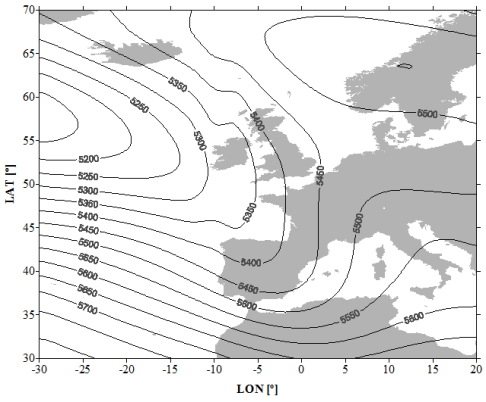
LAT [°]
LON [°]
70
65
60
55
50
45
40
35
30
-30
-25
-20
-15
-10
-5
0
5
10
15
20
5200
5250
5300
5350
5400
5450
5500
5550
5600
5650
5700
5800
5850
5900
5950
6000
6050
6100
6150
6200
6250
6300
6350
6400
6450
6500
6550
6600

Figure 4

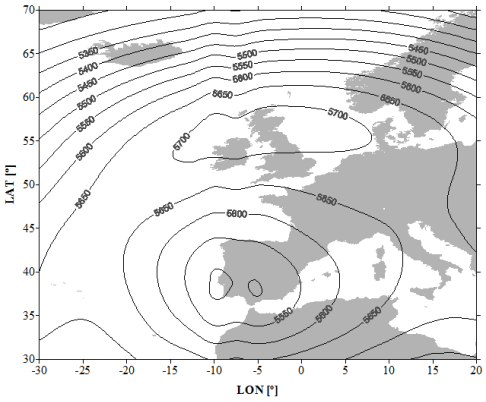
LAT [°]
LON [°]
70
65
60
55
50
45
40
35
30
-30
-25
-20
-15
-10
-5
0
5
10
15
20
5350
5400
5450
5500
5550
5600
5650
5700
5750
5800
5850
5900
5950
6000
6050
6100
6150
6200
6250
6300
6350
6400
6450
6500
6550
6600
6650
6700
6750
6800
6850

Figure 5

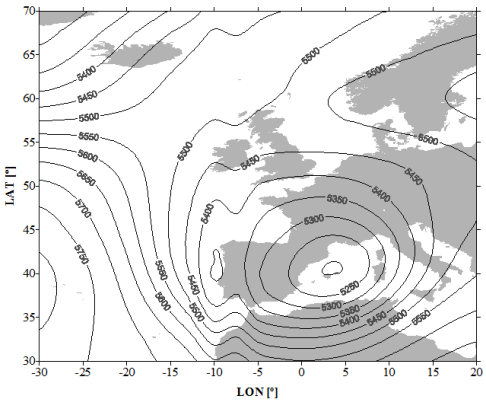
LAT [°]
LON [°]
70
65
60
55
50
45
40
35
30
-30
-25
-20
-15
-10
-5
0
5
10
15
20
5300
5350
5400
5450
5500
5550
5600
5650
5700
5750
5800
6500

Figure 6

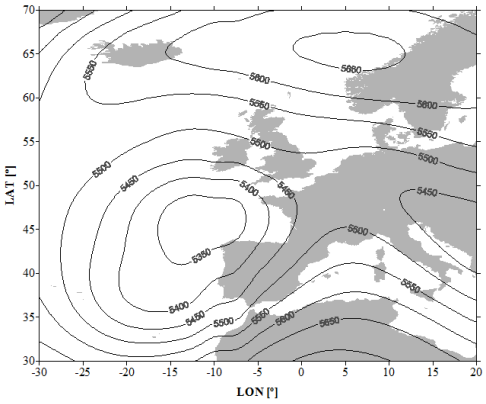
LAT [°]
LON [°]
70
65
60
55
50
45
40
35
30
-30
-25
-20
-15
-10
-5
0
5
10
15
20
5850
5900
5800
5750
5700
5650
5600
5550
5500
5450
5400
5350

Figure 7

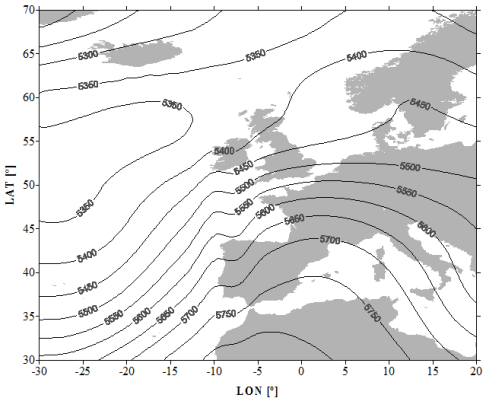
LAT [°]
LON [°]
70
65
60
55
50
45
40
35
30
-30
-25
-20
-15
-10
-5
0
5
10
15
20
5300
5350
5360
5400
5450
5500
5550
5600
5650
5700
5750
5800

Figure 8

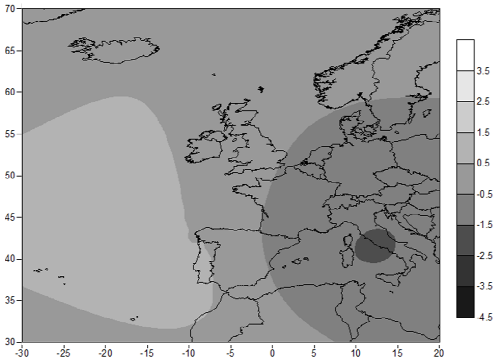
70
65
60
55
50
45
40
35
30
-30
-25
-20
-15
-10
-5
0
5
10
15
20
3.5
2.5
1.5
0.5
-0.5
-1.5
-2.5
-3.5
-4.5

Figure 9

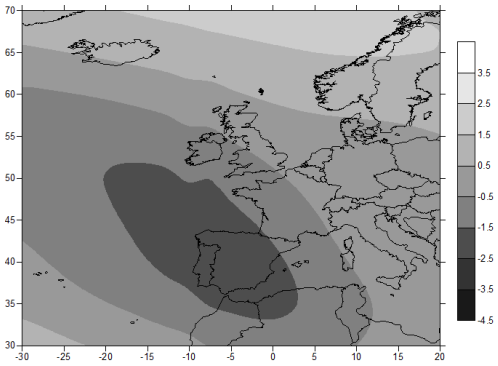
70
65
60
55
50
45
40
35
30
-30
-25
-20
-15
-10
-5
0
5
10
15
20
3.5
2.5
1.5
0.5
-0.5
-1.5
-2.5
-3.5
-4.5

Figure 10

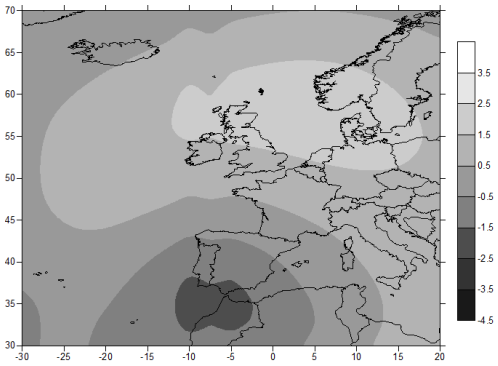
70
65
60
55
50
45
40
35
30
-30
-25
-20
-15
-10
-5
0
5
10
15
20
3.5
2.5
1.5
0.5
-0.5
-1.5
-2.5
-3.5
-4.5

Figure 11

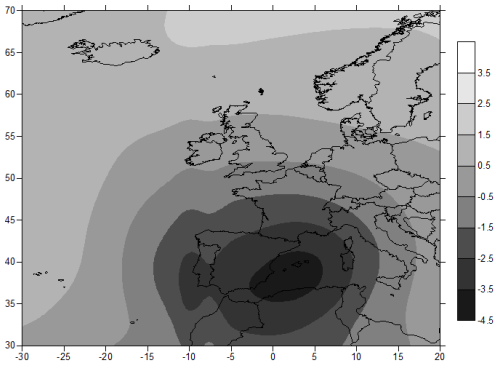
70
65
60
55
50
45
40
35
30
-30
-25
-20
-15
-10
-5
0
5
10
15
20
3.5
2.5
1.5
0.5
-0.5
-1.5
-2.5
-3.5
-4.5

Figure 12

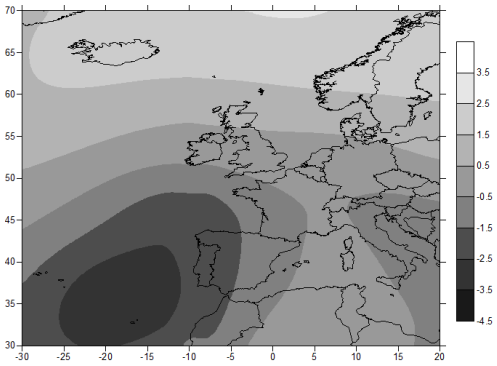
70
65
60
55
50
45
40
35
30
-30
-25
-20
-15
-10
-5
0
5
10
15
20
3.5
2.5
1.5
0.5
-0.5
-1.5
-2.5
-3.5
-4.5

Figure 13

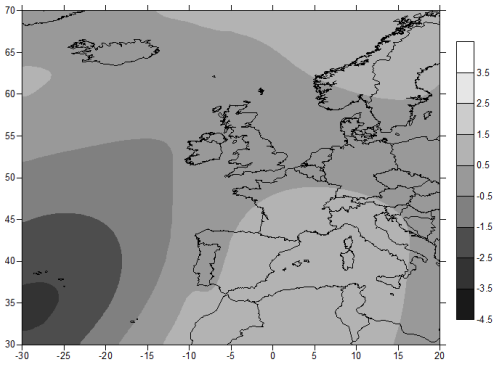
70
65
60
55
50
45
40
35
30
-30
-25
-20
-15
-10
-5
0
5
10
15
20
3.5
2.5
1.5
0.5
-0.5
-1.5
-2.5
-3.5
-4.5

Figure 14

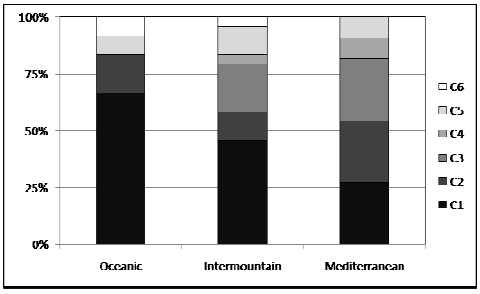
100%
75%
50%
25%
0%
Oceanic
Intermountain
Mediterrancan
C6
C5
C4
C3
C2
C1

Figure 15